International Journal of Physical Modelling in Geotechnics
Volume 14 Issue 3

LDFE study of bottom boundary effect in foundation model tests
Ullah, Hu, White and Stanier

International Journal of Physical Modelling in Geotechnics, 2014, **14**(3), 80–87
http://dx.doi.org/10.1680/ijpmg.14.00004
Paper 1400004
Accepted 05/03/2014 Revised 24/06/2014
Keywords: computational mechanics/foundations/offshore engineering

ice Institution of Civil Engineers
publishing

LDFE study of bottom boundary effect in foundation model tests

1 Shah Neyamat Ullah BSc
PhD Student, Centre for Offshore Foundation Systems, University of Western Australia, Crawley, WA, Australia

2 Yuxia Hu PhD
Professor, School of Civil and Resource Engineering, University of Western Australia, Crawley, WA, Australia

3 David White PhD
Winthrop Professor, Centre for Offshore Foundation Systems, University of Western Australia, Crawley, WA, Australia

4 Samuel Stanier PhD
Research Associate, Centre for Offshore Foundation Systems, University of Western Australia, Crawley, WA, Australia




Centrifuge model tests of deeply penetrating foundations have been widely used to assess the vertical bearing response, particularly in relation to the installation of spudcan foundations that support offshore drilling rigs. The potential influence of boundary effects owing to the proximity of these large foundations to the rigid base of the model container has not been previously addressed. In this study, large deformation finite-element (LDFE) analyses were conducted to assess the extent of the bottom boundary influence zone. Various foundation diameters were considered, with soil samples of sand overlying clay and uniform clay. The sand plug developed beneath the foundation is a major contributary factor to the boundary effect problem. The boundary effect is increased for sand over clay conditions, where a sand plug is entrapped beneath the foundation. The LDFE results were utilised to predict the thickness of the entrapped sand plug for different geometry and soil strength conditions. The results are distilled into a simple relationship that can be used to ascertain the bottom boundary influence zone when planning physical model tests and reinterpreting previous studies. The boundary influence zone predicted by the LDFE analysis agreed well with a corresponding centrifuge test.

Notation

D	spudcan diameter
d	spudcan penetration depth
d_{BE}	depth of boundary influence zone
d_b	spudcan position measured from the bottom of the container to the lowest widest part of the spudcan
d_{punch}	punch-through depth
g	acceleration due to gravity
H_{clay}	clay height
H_{plug}	sand plug height
H_s	sand thickness
h_{min}	minimum element size
I_D	relative density of sand
q_{nom}	nominal bearing resistance
s_u	undrained shear strength of clay
s_{uo}	strength of clay at sand–clay intercept
z	depth below the sand–clay intercept
γ'_c	effective unit weight of clay
γ'_s	effective unit weight of sand
δ	spudcan displacement increment
ρ	undrained shear strength gradient of clay with depth
ϕ	operative friction angle of sand
ϕ_{cv}	constant volume friction angle of sand
ψ	dilation angle of sand

1. Introduction

Offshore jack-up drilling rigs are generally supported on quasi-circular or polygonal foundations commonly referred to as spudcans. The prevalence of unexpected leg penetrations, often due to punch-through failure, has triggered research into spudcan deep penetration using physical modelling (Craig and Chua, 1990; Hossain *et al.*, 2005; Lee *et al.*, 2013a; Teh *et al.*, 2008).

Centrifuge tests are generally carried out in rectangular strong boxes or the channel of a drum centrifuge. The available depth of the strongbox or drum channel limits the range of soil heights and penetration depths that can be modelled. The measured penetration resistance will artificially rise as the spudcan approaches the bottom boundary (Figure 1). This bottom boundary influence zone can be larger for a soil profile with sand overlying clay because any trapped sand plug beneath the spudcan effectively deepens the foundation base. As a result of this boundary effect, a fictitious higher deep bearing resistance can be recorded, resulting in an underestimation of the punch-through depth (d_{punch}). It is therefore vital that the bottom boundary influence zone is correctly estimated when planning such tests, to avoid unwittingly mitigating the punch-through effect through an erroneous experimental effect.

The majority of previous research on boundary effects concerned cone penetration testing in a closed chamber (Bolton *et al.*, 1999; Phillips and Valsangkar, 1987; Schnaid and Houlsby, 1991). The effect of the boundary on dynamic loading in the centrifuge has also been investigated (Teymur and Madabhushi, 2003). This study specifically investigates the bottom boundary influence zone for spudcan foundations penetrating into soil profiles with sand over clay for a wide range of conditions. A simple relationship is established to indicate the bottom boundary influence zone. To achieve this, large deformation finite-element (LDFE) analysis incorporating the remeshing and interpolation technique with small strain model (RITSS) technique is employed (Hu and Randolph 1998a), and validated against an example centrifuge test. The LDFE/RITSS method was implemented in the FE package Afena (Carter and Balaam, 2006), which was originally developed at the University of Sydney.

2. LDFE problem description and model set-up

Figure 2 shows the model set-up of the LDFE/RITSS analyses. The spudcan diameters ranged from $D = 6$–16 m. The container depth was fixed at 30 m, which is typical for the strongboxes and g-levels used in previously published spudcan penetration tests at University of Western Australia (UWA) and other laboratories. Two-dimensional (2D) axisymmetric, six-noded triangular elements were used in all the analyses. A mesh and displacement increment sensitivity analysis was carried out to find the optimum mesh and spudcan displacement increment.

The mesh in all the analyses is broadly similar to Figure 2 with the spudcan displacement increment over diameter ratio (δ/D) ranging over $6{\cdot}25 \times 10^{-5}$ to $1{\cdot}66 \times 10^{-4}$, which is sufficiently small to give accurate results. To optimise the mesh after each remeshing stage h refinement cycles were implemented to discretise the soil domain in high shear strain regions (Hu and Randolph, 1998b). The minimum element size over foundation diameter ($h_{\min}/D$) varied as 0·0011–0·017.

The vertical boundaries along the centreline and far boundary were set up as rollers, and the bottom boundary was fixed in both horizontal and vertical directions. To focus on the bottom boundary effect, the lateral domain boundary was kept at a distance of $10D$ from the centre of the spudcan, which was found from additional analyses to be sufficient to remove any influence. To identify the bottom boundary effect, two parallel analyses were carried out for every soil profile as shown in Figure 1. First, the analysis was performed without any bottom boundary influence by keeping the bottom boundary

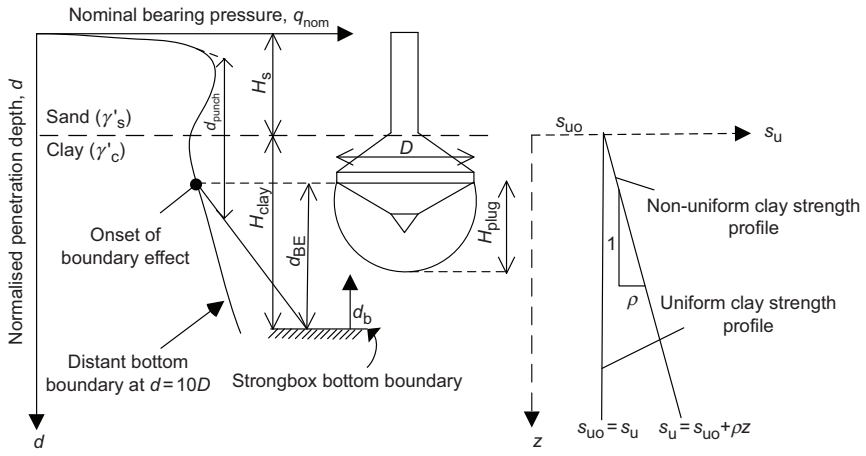

Figure 1. Problems definition: container boundary effect during spudcan penetration

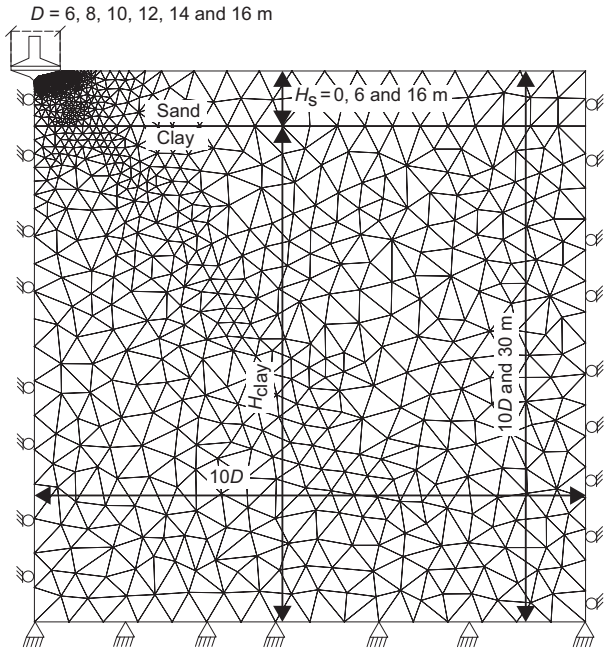

Figure 2. Model set-up and mesh at $d/D = 0$

at $10D$ from the domain surface (see Figure 1). Second, the analysis was performed with the bottom boundary placed at 30 m (i.e. ~$2D$–$5D$) from the domain surface, representing a rigid rough strongbox base. When comparing these parallel analyses, the point at which the responses diverge indicates the start of the bottom boundary influence zone (d_{BE}).

The thickness of the sand layer, H_s, was varied in the range 0, 6, 12 and 16 m with an effective unit weight (γ'_s) of 11 kN/m^3, and the undrained shear strength of the clay, s_u was set as 16·6, 50 and 100 kPa with an effective unit weight (γ'_c) of 6·5 kN/m^3. With different relative density, the effective unit weight of sand (γ'_s) varies over a narrow range. A collated list from the literature of sand effective unit weights in model centrifuge tests with varying relative density (I_D) of 58% to 99% was shown by Lee *et al.* (2013a: Table 2). This suggested effective unit weight of sand varying from 9·20 to 11·15 kN/m^3. The adopted value of 11 kN/m^3 is within this range. For even looser sand (I_D = 44%), Hu *et al.* (2014) measured an effective unit weight of 10 kN/m^3. The effective unit weight of clay (γ'_c) adopted coincides with the value reported in Teh *et al.* (2010) for UWA kaolin clay. The d_{BE} calculated is deemed to have negligible effect over these ranges of effective unit weights commonly tested by centrifuge modellers.

Using these parameters, the sand layer thickness to spudcan diameter ratios (H_s/D) covered a range of 0–2·0. Table 1 summarises all the cases analysed in this study. Both dense and loose sand, represented by different angles of friction and dilation, were considered.

A fully drained condition was maintained for the sand and a fully undrained condition for clay. Both materials were modelled as linear elastic-perfectly plastic obeying the Mohr–Coulomb (MC) failure criterion for sand and Tresca failure criterion for clay, with the parameters given in Table 1. The soil–spudcan interface in all the analyses was taken as fully rough, which is more onerous than a smooth interface with regard to boundary effect because the failure mechanism around the spudcan is larger.

3. LDFE/RITSS results against centrifuge test data

3.1 Spudcan penetration resistance

To validate the LDFE analysis approach, a centrifuge test result of spudcan penetration into sand over normally consolidated clay (Teh *et al.*, 2008) is shown in Figure 3 as curve A. In this instance the nominal bearing resistance q_{nom} is defined as the pressure obtained by dividing the total reaction force generated beneath the spudcan by the lower bottom widest area of the spudcan ($\pi D^2/4$). The high penetration resistance at deeper penetration depth was identified by Teh *et al.* (2008) as potentially a bottom boundary effect. For this test, H_s = 5 m, D = 6 m with a sand relative density (I_D) of 85%. The strength profile of the underlying clay had s_{uo} = 10 kPa (s_{uo} is the strength at the top of clay) and ρ = 1·20 kPa/m, where ρ is the shear strength gradient in clay (see Figure 1 for details noting that z is measured from the top of clay, note that $s_{uo} = s_u$ when $\rho = 0$). The sand constant volume friction angle (ϕ_{cv}) was reported as 34°. In the LDFE analysis, ϕ of 34° with dilation angle (ψ) of 4° was used for the sand. The sample depth (including the sand and clay layers) was 2·08D (12·5 m).

At shallow embedment, the LDFE analysis (curves B and C in Figure 3) does not reproduce the initial peak in resistance as the MC model does not simulate strain softening. However, the responses are wellmatched until the centrifuge test data diverge at $d_b/D \sim 0{\cdot}92$, indicating a potential bottom boundary effect (where d_b is the position of the spudcan measured from the bottom of the container to the lower bottom widest region of the spudcan). The LDFE analysis with the container base (case C) diverges slightly earlier at $d_b/D \sim 1{\cdot}06$, but the divergence accelerates slightly afterwards, close to $d_b/D \sim 0{\cdot}92$. This confirms that the divergence is associated with a bottom boundary effect and the LDFE and centrifuge data agree well.

An LDFE analysis with higher angles of friction and dilation (ϕ = 37°, ψ = 8°) is also shown in Figure 3. The peak resistance is still lower than the centrifuge measurement, indicating that the dilatancy of the sand in the centrifuge test was likely greater than 8°, although only briefly at peak resistance. The bottom

Case identifier	Thickness of sand, H_s: m	Operative friction angle: φ	Dilation angle: ψ	Undrained shear strength of clay, s_{uo}: kPa	Shear strength gradient, ρ: kPa/m	Spudcan diameter, D: m	Total depth H_{total}: m	Comments
Case 0	5	34°	4°	10	0·1,0·5, 1·20[a],1·50 and 2	6	12·5 and 10D	Comparison with centrifuge test and effect of clay strength gradient on plug development and boundary effect
Case I	6	31°	2°	16·6	0	8,10,12,14,16	30 and 10D	Loose sand on uniform clay
Case II	6	38°	8°	16·6	0	8,10,12,14,16	30 and 10D	Dense sand on uniform clay: effect of dense sand on plug development and boundary effect
Case III	16	31°	2°	16·6	0	8,10,12,14,16	30 and 10D	Loose sand on uniform clay: effects of higher sand thickness on sand plug and boundary effect
Case IV	0	—	—	16·6	0	6	30 and 10D	Uniform clay: effect of bottom boundary when no plug is entrapped
Case V	6	31°	2°	16·6, 50, 100	0	10	10D	Sand on clay: effect of s_u on plug development
Case VI	6 and 12	31°	2°	50, 100	0	6	10D	Sand on clay: plug development in thicker sand and stiff clay

[a]Centrifuge test case

Table 1. Summary of LDFE analyses undertaken

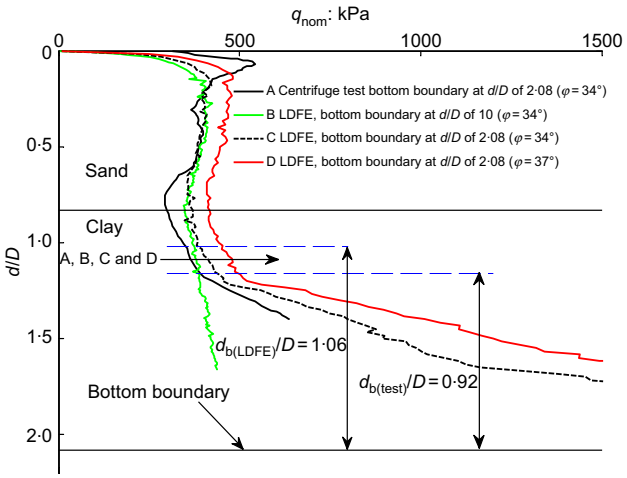

Figure 3. Comparison between LDFE results and centrifuge test using clay with strength increasing with depth

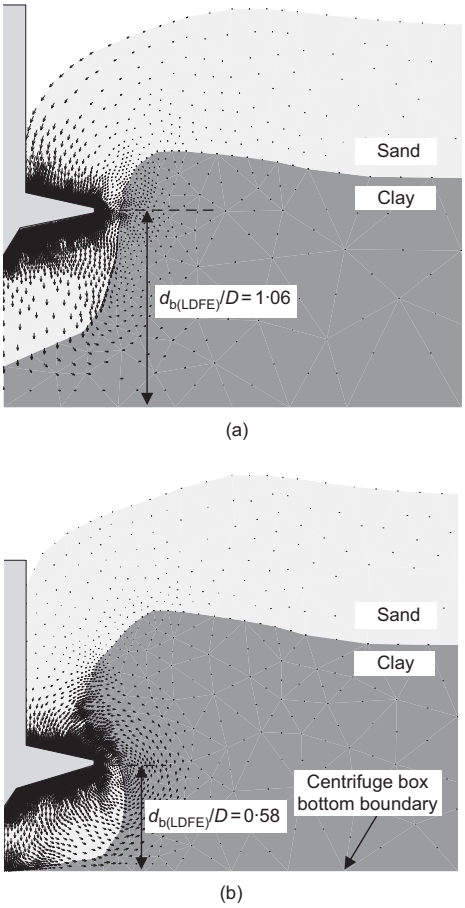

Figure 4. Soil displacement vectors for curve C at (a) $d_{b(LDFE)}/D$ = 1·06, (b) $d_{b(LDFE)}/D$ = 0·58 using clay with strength increasing with depth

boundary effect is evident at the same depth. This is because although curve D corresponds to a higher friction angle, the entrapped sand plug had similar geometry. Both curves C and D recorded a plug depth of ~5 m, which also agrees well with the centrifuge test by Teh *et al.* (2008). It can be concluded that the bottom boundary effect is not significantly influenced by the frictional properties of the top sand layer. Other comparisons between case I and case II of Table 1 show the same trend.

3.2 Soil flow mechanisms near bottom boundary

Figure 4(a) and 4(b) depict the soil flow mechanisms when the spudcan approaches the bottom boundary. Figure 4(a) shows that at d_b/D = 1·06 of curve C in Figure 3, where the bottom boundary effect initiates, the entrapped sand plug is moving downwards with essentially rigid body motion. At d_b/D = 0·58 (Figure 4(b)), squeezing of the sand plug between the spudcan and the bottom boundary is evident, leading to horizontal movement within the plug.

To illustrate these mechanisms more clearly, contours of the horizontal soil velocity normalised by the spudcan speed are compared for cases B and C in Figure 3 (i.e. without and with the bottom boundary influence) at d/D = 1·67 (Figure 5(a) and 5(b) respectively). When the boundary is remote (Figure 5(a)) the soil flow mechanism is essentially symmetrical about a horizontal plane at the mid-depth of the plug. However, when the bottom boundary is close (Figure 5(b)), the flow is strongly asymmetric, with the flow mechanism below the spudcan being distorted by the rigid bottom boundary. This distortion of the soil flow away from the optimal geometry of mechanism increases the penetration resistance. Similar observations were made for the sand over uniform clay scenarios but detailed soil flow mechanisms are not reported here.

These observations highlight the important influence of the sand plug on the onset of a bottom boundary effect. To estimate the boundary influence zone for practical applications it is therefore important to predict the thickness of this plug for different values of normalised sand layer thickness (H_s/D) and undrained clay strength (s_u).

4. Results of parametric LDFE/RITSS study

4.1 Sand plug height (H_{plug})

All the LDFE/RITSS analyses performed are summarised in Table 1. The stabilised sand plug height (H_{plug}/D) derived from the LDFE results is compared against the initial sand layer thickness H_s/D in Figure 6(a). H_{plug} is measured as the sand plug formed, whereas the spudcan was embedded into the clay

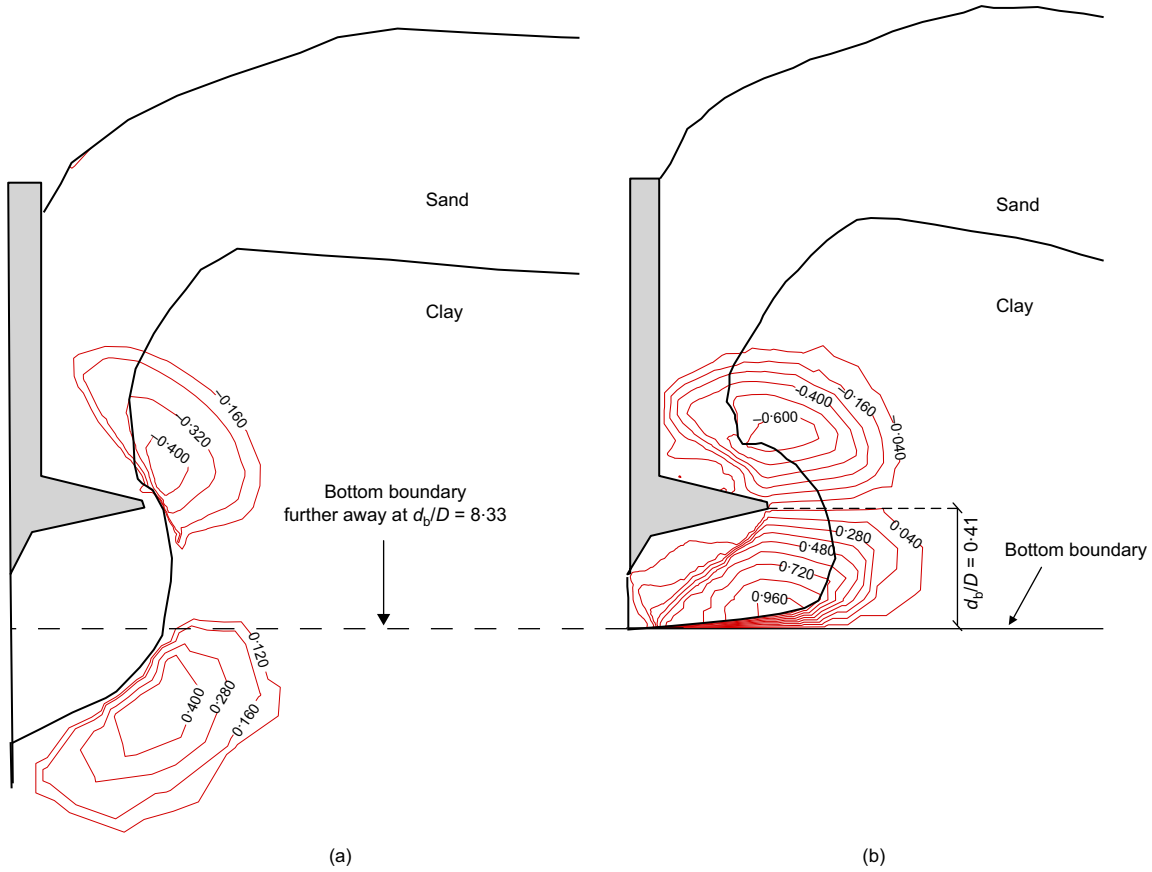

Figure 5. Incremental normalised horizontal velocity contours at d/D = 1·67: (a) curve B and (b) curve C using clay with increasing strength with depth

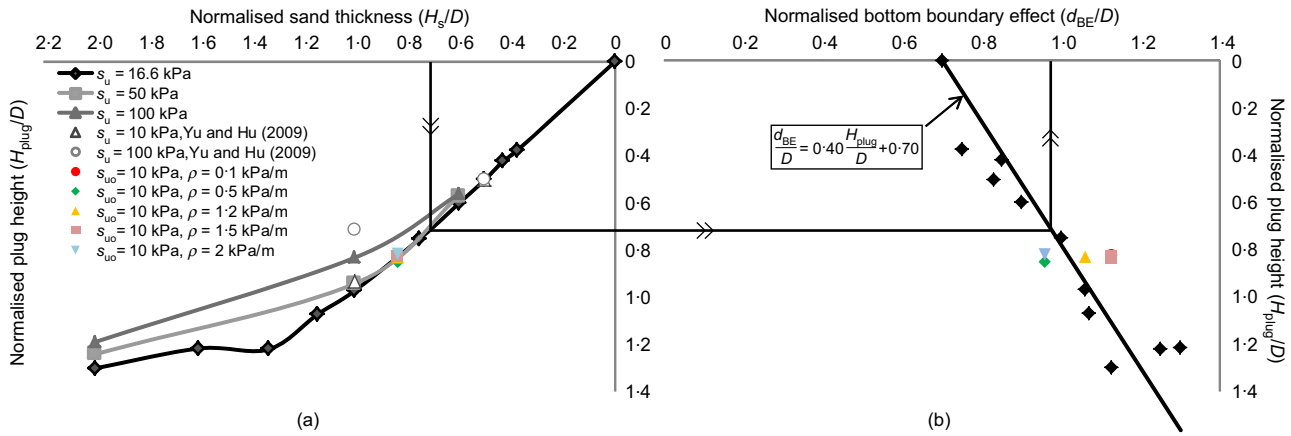

Figure 6. Collated results and procedure for estimation of bottom boundary influence zone

prior to any plug distortion induced by the bottom boundary. The origin in Figure 6(a) refers to the uniform clay case (case IV of Table 1) where no sand plug is formed. For all the cases with s_u = 16·6 kPa, the plug height H_{plug}/D increases linearly with the sand layer thickness H_s/D when $H_s/D \leq 1{\cdot}30$. When the sand layer thickness is beyond $H_s/D = 1{\cdot}30$, the sand plug height approaches a limit of $H_{plug}/D \sim 1{\cdot}20$.

To investigate the effect of clay strength, additional cases considered s_u = 50 and 100 kPa. When the sand layer is thin ($H_s/D < 1{\cdot}0$ for s_u = 50 kPa, $H_s/D < 0{\cdot}6$ for s_u = 100 kPa), the relationship between H_s/D and H_{plug}/D is still linear. However, when the sand layer becomes thicker, stiffer clay causes some of the plug material to flow around the spudcan and the plug height reduces accordingly. Previous LDFE (Yu and Hu, 2009) and centrifuge test results (Teh *et al.*, 2008) are also plotted in Figure 6(a), showing good agreement.

For sand over clay with strength increasing with depth, the LDFE analysis shown in Figure 3 was repeated for different strength gradients (ρ) as 0·1, 0·5, 1·20 (centrifuge test ρ), 1·5 and 2 kPa/m, which span the plausible ranges (e.g. Lee *et al.*, 2013b; Teh *et al.*, 2008). The H_{plug} measurements in these tests were identical and were close to the initial H_s, with bottom boundary influence zone (d_{BE}) only varying slightly. The clay strength gradient therefore has negligible impact on the influence zone at least over the range studied here (0·1~2 kPa/m). The sand plug height obtained from the weaker clay provides an upper bound for estimation of the plug thickness and therefore the bottom boundary influence zone d_{BE}.

4.2 Design chart of d_{BE}

As depicted in Figure 1, the sand plug, once its size is stabilised in the lower clay layer, behaves as part of the foundation penetrating into the clay. As the base of the plug approaches the bottom boundary, it is felt by the spudcan. The bottom boundary influence zone (d_{BE}/D) increases with the plug height (H_{plug}/D).

The relationship is displayed in Figure 6(b), which presents the values of d_{BE}/D determined from all the parallel LDFE analyses listed in Table 1 with near and far container bottom boundaries (i.e. container depths of 30 m and 10D). For the uniform clay case, $d_{BE}/D = 0{\cdot}7$ represents the plastic flow mechanism around the spudcan and any further penetration causes yielding at the boundary nodes. As d_{BE}/D does not increase proportionally with H_{plug}/D, this indicates that the flow mechanism around the combined spudcan–plug foundation is a different shape to the flow around a spudcan alone. This is to be expected, as the plug has a rounded base, compared to the flatter spudcan base (Figure 4(a)). d_{BE}/D increases in proportion to $\sim 0{\cdot}4H_{plug}/D$, and so the bottom boundary influence zone can be estimated as (Figure 6)

$$1. \quad \frac{d_{BE}}{D} = 0{\cdot}40\frac{H_{plug}}{D} + 0{\cdot}70;\ 0 \leq \frac{H_s}{D} \leq 2$$

5. Conclusion

To assess the potential influence of boundary effects in model tests of deeply penetrating foundations, the bottom boundary influence zone has been explored using large deformation finite-element analysis. Penetration resistance profiles of a spudcan on sand over uniform clay soils in containers of different depths were used to identify the bottom boundary influence zone. Key conclusions are outlined below.

(*a*) When a spudcan penetrates into a soil profile with sand over clay, there is always a sand plug formed underneath the spudcan which is carried down into the clay layer. The stabilised sand plug size increased approximately linearly with the sand layer thickness until a limit of $H_{plug}/D = 1{\cdot}2$ at $H_s/D = 1{\cdot}3$. With further increase in sand layer thickness, the sand plug height change was minimal.

(*b*) The shear strength of the clay layer showed a small influence on the sand plug height, with the sand plug thickness decreasing slightly with increased shear strength in the clay.

(*c*) The stabilised sand plug underneath the spudcan effectively increased the spudcan depth, but also changed the shape of the flow mechanism. The bottom boundary influence zone was 0·7D for uniform clay, and was increased by 40% of the normalised plug (H_{plug}/D) thickness (not 100% – owing to the changing flow mechanism) for the sand over clay cases.

(*d*) These effects lead to a simple relationship between the normalised sand layer thickness (H_s/D), the normalised sand plug height (H_{plug}/D), and the normalised bottom boundary influence zone (d_{BE}/D).

This simple relationship enables the bottom boundary influence zone to be assessed when planning centrifuge model tests in uniform clay and on sand overlying normally consolidated or uniform strength clay. It also allows the potential influence that bottom boundary effects may have had on previously published studies to be identified.

Acknowledgements

The work forms part of the activities of the Centre for Offshore Foundation Systems (COFS) at the University of Western Australia, which is supported by the Lloyd's Register Foundation as a Centre of Excellence and is a part of the Australian Research Council (ARC) Centre of Excellence in Geotechnical Science and Engineering. The authors also acknowledge the financial contribution of the Australian Research Council (ARC) through Discovery project No. DP1096764. The third author is

supported by the Shell Energy and Minerals Institute (EMI) Chair in Offshore Engineering.

REFERENCES

Bolton MD, Gui MW, Garnier J, Corte JF, Bagge G, Laue J and Renzi R (1999) Centrifuge cone penetration tests in sand. *Géotechnique* **49(4)**: 543–552.

Carter JP and Balaam NP (2006) *AFENA User Manual Version 6*. Centre for Geotechnical Research, University of Sydney, Sydney, Australia.

Craig WH and Chua K (1990) Deep penetration of spudcan foundations on sand and clay. *Géotechnique* **40(4)**: 541–556.

Hossain MS, Hu Y, Randolph MF and White DJ (2005) Limiting cavity depth for spudcan foundations penetrating clay. *Géotechnique* **55(9):** 679–690.

Hu Y and Randolph MF (1998a) A practical numerical approach for large deformation problems in soil. *International Journal for Numerical and Analytical Methods in Geomechanics* **22(5)**: 327–350.

Hu Y and Randolph MF (1998b) H-adaptive FE analysis of elasto-plastic non homogeneous soil with large deformation. *Computers and Geotechnics* **23(1/2)**: 61–83.

Hu P, Stanier S, Cassidy M and Wang D (2014) Predicting peak resistance of spudcan penetrating sand overlying clay. *Journal of Geotechnical and Geoenvironmental Engineering* **140(2)**, http://dx.doi.org/10.1061/(ASCE)GT.1943-5606.0001016.

Lee KK, Randolph MF and Cassidy MJ (2013a) Bearing capacity on sand overlying clay soils: a simplified conceptual model. *Géotechnique* **63(15)**: 1285–1297.

Lee KK, Cassidy MJ and Randolph MF (2013b) Bearing capacity on sand overlying clay soils: experimental and finite element investigation of potential punch-through failure. *Géotechnique* **63(15)**: 1271–1284.

Phillips R and Valsangkar AJ (1987) *An Experimental Investigation of Factors Affecting Penetration Resistance in Granular Soils in Centrifuge Modelling*. Cambridge University Engineering Department, Cambridge, UK, Technical Report No. 210.

Schnaid F and Houlsby GT (1991) An assessment of chamber size effects in calibration of in situ tests in sand. *Géotechnique* **41(3)**: 437–445.

Teh KL, Cassidy MJ, Leung CF, Chow YK, Randolph MF and Quah CK (2008) Revealing the bearing capacity mechanisms of a penetrating spudcan through sand overlying clay. *Géotechnique* **58(10)**: 793–804.

Teh KL, Leung CF, Chow YK and Cassidy MJ (2010) Centrifuge model study of spudcan penetration in sand overlying clay. *Géotechnique* **60(11)**: 825–842.

Teymur B and Madabhushi SPG (2003) Experimental study of boundary effects in dynamic centrifuge modelling. *Géotechnique* **53(7)**: 655–663.

Yu L and Hu Y (2009) Spudcan penetration in loose sand over uniform clay. *Proceedings of the ASME 28th International Conference on Ocean, Offshore and Arctic Engineering*, *Honolulu*, *HI*, *USA*, vol. 7, pp. 195–201.